Original Article

The role of ^{18}F-FDG PET/CT metabolic parameters in the differential diagnosis of post-transplant lymphoproliferative disorder after pediatric liver transplantation

Chaoran Wang[#], Guanyun Wang[#], Wei Wang, Ying Kan, Mingyu Zhang, Jigang Yang

Department of Nuclear Medicine, Beijing Friendship Hospital, Capital Medical University, Beijing, China

Contributions: (I) Conception and design: C Wang, G Wang; (II) Administrative support: J Yang, W Wang, Y Kan, M Zhang; (III) Provision of study materials or patients: C Wang, G Wang, J Yang; (IV) Collection and assembly of data: C Wang; (V) Data analysis and interpretation: C Wang, G Wang; (VI) Manuscript writing: All authors; (VII) Final approval of manuscript: All authors.

[#]These authors contributed equally to this work.

Correspondence to: Jigang Yang, MD, PhD. Department of Nuclear Medicine, Beijing Friendship Hospital, Capital Medical University, No. 95 Yong'an Road, Xicheng District, Beijing 100050, China. Email: yangjigang@ccmu.edu.cn.

Background: Post-transplant lymphoproliferative disorder (PTLD) is a significant complication after liver transplantation. Research on the diagnostic value of the Fluorine-18 fluorodeoxyglucose positron emission tomography/computerized tomography (^{18}F-FDG PET/CT) metabolic parameters of PTLD in pediatric liver transplantation (pLT) recipients is limited. This study sought to evaluate the diagnostic efficacy of ^{18}F-FDG PET/CT in differentiating between PTLD and non-PTLD lymphadenopathy in pLT recipients.

Methods: This retrospective study collected the ^{18}F-FDG PET/CT scans with clinical and pathological information of all consecutive children who were clinically suspected of PTLD from November 2016 to September 2022 at the Beijing Friendship Hospital. The ^{18}F-FDG PET/CT metabolic parameters of the two groups were analyzed. We then established a diagnostic model composed of the clinical characteristics and metabolic parameters.

Results: In total, 57 eligible patients were enrolled in this study, of whom 40 had PTLD and 17 had non-PTLD lymphadenopathy. Of the metabolic parameters examined in this study, total lesion glycolysis (TLG) had the highest area under the curve (AUC) value [0.757, 95% confidence interval (CI): 0.632–0.883, P=0.002]. The AUCs of the other metabolic parameters were all less than the AUC of TLG, including the maximum standardized uptake value (SUV_{max}) (AUC: 0.725, 95% CI: 0.597–0.853, P=0.008), mean standardized uptake value (SUV_{mean}) (AUC: 0.701, 95% CI: 0.568–0.834, P=0.017), metabolic tumor volume total (MTV_{total}) (AUC: 0.688, 95% CI: 0.549–0.827, P=0.040), TLG total (AUC: 0.674, 95% CI: 0.536–0.812, P=0.026). The diagnostic model, which was composed of clinical characteristics (digestive symptoms), the SUV_{max}, TLG, and the MTV_{total}, showed excellent performance in the differential diagnosis (sensitivity: 0.675, 95% CI: 0.508–0.809; specificity: 0.941, 95% CI: 0.692–0.997; positive predictive value: 0.964, 95% CI: 0.798–0.998; and negative predictive value: 0.552, 95% CI: 0.360–0.730).

Conclusions: The ^{18}F-FDG PET/CT metabolic parameters can be used to distinguishing between PTLD and non-PTLD lymphadenopathy in pLT recipients.

Keywords: Fluorine-18 fluorodeoxyglucose positron emission tomography/computerized tomography (^{18}F-FDG PET/CT); metabolic parameters; differential diagnosis; pediatric; liver transplant

Submitted Jul 26, 2023. Accepted for publication Nov 17, 2023. Published online Jan 05, 2024.
doi: 10.21037/qims-23-1059
View this article at: https://dx.doi.org/10.21037/qims-23-1059

Introduction

Post-transplant lymphoproliferative disorder (PTLD) is a significant complication after liver transplantation. PTLD encompasses a heterogeneous and potentially fatal group of malignant or pre-malignant lesions that range from benign lymphoproliferative disorders to aggressive lymphomas (1). Compared to adults, children have a higher risk of developing PTLD, and the incidence of PTLD among pediatric liver transplantation (pLT) recipients is 4.7–14.5% (2,3). Epstein-Barr virus (EBV) infection is believed to play a crucial role in pediatric PTLD development (4,5). In children with PTLD, lymphadenopathy is a common clinical symptom, and may be accompanied by other manifestations, including organ dysfunction, B symptoms, and allograft involvement (5,6). However, lymphadenopathy is a frequent and non-specific sign in healthy or sick children, and pediatric lymphadenopathy is benign in most patients (7-10).

Due to the significant differences in treatment methods for PTLD and non-PTLD lymphadenopathy, the differential diagnosis of PTLD and non-PTLD lymphadenopathy is crucial (10,11). The current diagnostic approach for PTLD relies on pathological examination (12). Unfortunately, not every pLT recipient suspected of PTLD can undergo biopsy due to its invasiveness, high cost, and potential complications (13-15). The use of the EBV-DNA viral load as a potential biomarker for PTLD diagnosis is limited by the kind of specimens required, the time of detection, its threshold value, and its low specificity in clinical application (16-21). Therefore, it is imperative to explore more effective and non-invasive approaches for discriminating between PTLD and non-PTLD lymphadenopathy.

Fluorine-18 fluorodeoxyglucose positron emission tomography/computerized tomography (^{18}F-FDG PET/CT) has been widely employed in the detection, staging, and assessment of treatment responses in PTLD (22-29). However, research on the differential diagnostic value of the ^{18}F-FDG PET/CT metabolic parameters of PTLD and non-PTLD lymphadenopathy in pLT recipients is limited. This study sought to evaluate the differential diagnostic efficacy of ^{18}F-FDG PET/CT metabolic parameters for distinguishing between PTLD and non-PTLD lymphadenopathy in pLT recipients with suspected PTLD. We present this article in accordance with the STARD reporting checklist (available at https://qims.amegroups.com/article/view/10.21037/qims-23-1059/rc).

Methods

Patients

We retrospectively collected the ^{18}F-FDG PET/CT scans of all consecutive pLT recipients (aged ≤18 years) who were clinically suspected of PTLD at the Beijing Friendship Hospital, Capital Medical University from November 2016 to September 2022. The ^{18}F-FDG PET/CT indications for patients were as follows: lymphadenopathy; appearance of suspicious symptoms, such as unexplained digestive symptoms (including abdominal pain, diarrhea, vomiting, and bloating), anemia, B symptoms (including weight loss >10%, night sweats, and a body temperature >38 ℃), and suspicious lesions found by ultrasound. For patients who underwent series ^{18}F-FDG PET/CT, only their first scan was included in the study. For patients who underwent a secondary liver transplantation, the most recent date of transplantation was used for further analysis (30). Patients were excluded from the study if they met any of the following exclusion criteria: (I) had incomplete clinical or imaging data; (II) had a confirmed second malignancy that might interfere with the results; (III) had received preemptive PTLD treatment before imaging; (IV) had poor quality images; (V) a non-PTLD patient with a follow-up period <2 years after the pathological examination (24,31). Data were collected from the electronic patient files, including demographic information, clinical history, and biopsy details; the biopsies were planned after imaging and diagnosis.

The study was conducted in accordance with the Declaration of Helsinki (as revised in 2013). The study was approved by the Research Ethics Committee of the Beijing Friendship Hospital, Capital Medical University, and the requirement of individual consent for this retrospective analysis was waived.

Reference standard

All the patients were diagnosed by pathological examination. Pathological specimens were obtained through surgical resection or fine needle aspiration, and the diagnoses were confirmed by at least two pathologists, who were blinded to the ^{18}F-FDG PET/CT results. EBV-encoded RNA (EBER) *in situ* hybridization was performed to confirm the presence of EBV (32). All the PTLD cases were classified according to World Health Organization 2017 classification (33).

Image acquisition

All the patients underwent ^{18}F-FDG PET/CT (Siemens Biograph mCT, Germany) according to the recommended protocol of the manufacturer. The patients were instructed to fast at least 4 hours to ensure they had a glucose level lower than 11.1 mmol/L, and were then subsequently injected with ^{18}F-FDG (3.7 MBq/kg). The whole-body scans were acquired from the skull base to the upper femur approximately 1 hour after the injection. Children who could not remain still during the imaging process were given chloral hydrate for sedation half an hour prior to scanning (0.5 mg/kg, upper limit: 20 mg). The low-dose CT was performed for attenuation correction and anatomical reference with the following parameters: tube voltage: 120 kV; tube current: 160 mAs; pitch: 0.55; layer thickness: 3 mm; and reconstructed increment: 2 mm. The PET images were acquired for 2 min/bed position and were reconstructed using the ordered subset expectation maximization algorithm.

Image analysis

All the ^{18}F-FDG PET/CT images were reviewed by two experienced nuclear medicine physicians, who were blinded to the pathological data, at a workstation. Consensus meetings were held to resolve any controversial diagnoses (25). Positive lesions were defined as focal areas exhibiting increased ^{18}F-FDG uptake that were not associated with physiological distribution or non-PTLD pathologies (25,31). The volume of interest (VOI) was outlined by spherical volumes, and the threshold was set at 41% of the maximum standardized uptake value (SUV_{max}) of VOI according to the European Association of Nuclear Medicine because of its satisfactory inter-observer reproducibility (34,35). The metabolic parameters, including SUV_{max}, mean standardized uptake value (SUV_{mean}), peak standardized uptake value (SUV_{peak}), metabolic tumor volume (MTV), and total lesion glycolysis (TLG) (which was calculated as the $SUV_{mean} \times MTV$), were calculated from the lesion, with the SUV_{max} higher than other lesions in each patient. By summing the MTV and TLG from all the positive lesions, the MTV total (MTV_{total}) and TLG total (TLG_{total}) were also calculated (36). When calculating the metabolic parameters for the whole body, only focal uptake was considered indicative of bone marrow involvement, while diffuse involvement was excluded from consideration (37). Diffuse splenic uptake exceeding 150% of the hepatic background or any focal lesion in the spleen was considered splenic disease (37).

Statistical analysis

The qualitative variables are described as the count and percentage [n (%)], and were compared using the Chi-squared test. The normality of the continuous variables was determined by the Shapiro-Wilk test. Normally distributed continuous variables are expressed as the mean ± standard deviation, and skewed distributed continuous variables are expressed as the median with the interquartile range. Comparisons of the continuous variables between PTLD and non-PTLD lymphadenopathy were performed using the Mann-Whitney test or student *t*-test. The area under the receiver operating characteristic (ROC) curves (AUC) was calculated to evaluate the predictive value of ^{18}F-FDG PET/CT. The sensitivity, specificity, positive predictive value (PPV), and negative predictive value (NPV) of the metabolic parameters were computed with 95% confidence intervals (CIs). Multivariable logistics regression models were built to discriminate between PTLD and non-PTLD lymphadenopathy. The maximum AUC was the basis for determining the best model, and the model not only included both the clinical and metabolic parameters, but also reflected the hottest lesion and whole-body situation. The Delong test was conducted using the R software pROC package (https://CRAN.R-project.org/package=pROC) to test differences between ROC curves. To compare the diagnostic values of different models, integrated discriminatory improvement (IDI) and net reclassification improvement (NRI) were computed using the R software PredictABEL package (https://CRAN.R-project.org/package=PredictABEL). The threshold for significance was set at P=0.05. The statistical analysis was carried out using SPSS Statistics 26 (IBM, Armonk, USA) and R software version 4.0.2 (Bell Laboratories, USA).

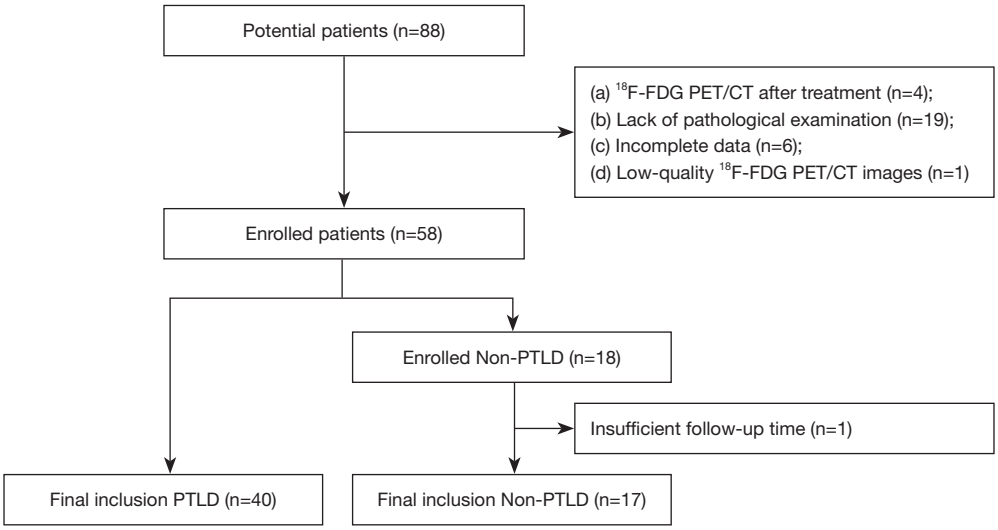

Figure 1 Flowchart of the patient inclusion and exclusion process. ^{18}F-FDG PET/CT, fluorine-18 fluorodeoxyglucose positron emission tomography/computerized tomography; PTLD, post-transplant lymphoproliferative disorder.

Results

Clinical characteristics

A total of 88 potential pLT recipients were identified. After screening, 57 eligible pLT patients were enrolled in this retrospective study, of whom 40 had PTLD and 17 had non-PTLD lymphadenopathy (*Figure 1*). The clinical characteristics of the patients in the PTLD and non-PTLD groups are set out in *Table 1*. In relation to the demographic data, age at the time of liver transplantation or at the time PTLD was suspected, and the time from liver transplantation to PTLD was suspected did not differ significantly between the PTLD and non-PTLD groups; however, gender differed significantly between the two groups [boy:girl, 18 (45%):22 (55%) *vs.* 13 (76.5%):4 (23.5%), respectively, P=0.029]. In relation to the clinical characteristics, digestive symptoms were more common in PTLD patients than non-PTLD patients [18 (45%) *vs.* 2 (12%), respectively, P=0.016]. Conversely, no significant difference in the percentages of patients with other symptoms, including anemia, B symptoms, and lymphadenopathy, was observed between the PTLD and non-PTLD groups. In relation to the pathological examinations, 15 (88%) patients had reactive lymphoid hyperplasia and 2 (12%) patients had dermatopathic lymphadenitis in the non-PTLD group, while 30 (75%) patients had non-destructive PTLD, 6 (15%) patients had polymorphic PTLD, 2 (5%) patients had monomorphic PTLD, and 2 (5%) patients had classical Hodgkin's lymphoma-like PTLD in the PTLD group. In addition, more patients were EBER positive in the PTLD group than in the non-PTLD group [38 (95%) *vs.* 10 (59%), respectively, P=0.002].

Comparison of the ^{18}F-FDG PET/CT metabolic parameters between the PTLD group and non-PTLD group

The ^{18}F-FDG PET/CT findings are set out in *Table 2*. The majority of the metabolic parameters, including the SUV_{max} [5.8 (3.3–7.9) *vs.* 3.5 (2.9–4.3), respectively, P=0.008], the SUV_{mean} [3.4 (2.1–4.9) *vs.* 2.2 (1.9–2.8), respectively, P=0.017], TLG [9.9 (5.7–29.1) *vs.* 5.0 (3.0–7.8), respectively, P=0.002], the MTV_{total} [27.4 (14.3–62.2) *vs.* 18.0 (12.0–24.3), respectively, P=0.040], and the TLG_{total} [54.2 (29.5–181.8) *vs.* 36.0 (22.5–43.5), respectively, P=0.026], were higher in the PTLD patients than non-PTLD patients. There were no statistically significant differences in the SUV_{peak} or MTV between the two groups.

The differential diagnostic performance of the ^{18}F-FDG PET/CT metabolic parameters in the PTLD group and non-PTLD group

The performance results of ^{18}F-FDG PET/CT for differential diagnosis are presented in *Table 3*. The ROC curves showed that TLG had the highest diagnostic

Table 1 The clinical characteristics of the PTLD and non-PTLD groups

Characteristic	PTLD (n=40)	Non-PTLD (n=17)	P
Age at the time PTLD was suspected (years)	3.1 (2.1–3.8)	2.7 (2.1–4.9)	0.958
Age at the time of liver transplantation (years)	1.0 (0.6–1.9)	0.7 (0.5–1.1)	0.129
Boy:girl	18 [45]:22 [55]	13 [76.5]:4 [23.5]	0.029
Clinical data			
Time from liver transplantation to PTLD was suspected (days)	414.0 (219.5–781.8)	635.0 (390.0–1,193.5)	0.118
Clinical symptoms			
Digestive symptoms	18 [45]	2 [12]	0.016
Anemia	14 [35]	1 [6]	0.051
B symptoms	15 [38]	4 [24]	0.306
Lymphadenopathy	34 [85]	17 [100]	0.091
Biopsied lesions			
Cervical lymph nodes	33 [82.5]	14 [82]	
Inguinal lymph nodes	2 [5]	1 [6]	
Abdominal lymph nodes	1 [2.5]	1 [6]	
Axillary lymph nodes	0 [0]	1 [6]	
Digestive tract	3 [7.5]	0	
Liver	1 [2.5]	0	
Pathologic findings			
EBER positive	38 [95]	10 [59]	0.002
Non-PTLD			
Reactive lymphoid hyperplasia	–	15 [88]	
Dermatopathic lymphadenitis	–	2 [12]	
PTLD			
Non-destructive PTLD	30 [75]	–	
Polymorphic PTLD	6 [15]	–	
Monomorphic PTLD	2 [5]	–	
cHL PTLD	2 [5]	–	

Data are presented as number [percentage] or median (interquartile range). B symptoms, including weight loss >10%, night sweats, and a body temperature >38 ℃. PTLD, post-transplant lymphoproliferative disorder; EBER, Epstein-Barr virus encoded RNAs; cHL PTLD, classical Hodgkin's lymphoma-like PTLD.

efficacy in differentiating between PTLD and non-PTLD lymphadenopathy, with cut-off value of 6.08 and an AUC of 0.757 (95% CI: 0.632–0.883). TLG had an accuracy of 0.719 (95% CI: 0.585–0.830), a sensitivity of 0.725 (95% CI: 0.559–0.849), a specificity of 0.706 (95% CI: 0.440–0.886), a PPV of 0.853 (95% CI: 0.682–0.945), and a NPV of 0.522 (95% CI: 0.311–0.726). A multivariate logistic regression was then conducted to establish the following differential diagnostic model: digestive symptoms plus SUV_{max} plus TLG plus MTV_{total}. The model had an AUC of 0.868 (95% CI: 0.769–0.966), an accuracy of 0.754 (95% CI: 0.622–0.859), a sensitivity of 0.675 (95% CI: 0.508–0.809), a specificity of 0.941 (95% CI: 0.692–0.997), a PPV of 0.964 (95% CI: 0.798–0.998), and a NPV of 0.552 (95% CI:

Table 2 The value of the ^{18}F-FDG PET metabolic parameters between the PTLD and non-PTLD groups

Variable	PTLD	Non-PTLD	P
SUV_{max}	5.8 (3.3–7.9)	3.5 (2.9–4.3)	0.008
SUV_{mean}	3.4 (2.1–4.9)	2.2 (1.9–2.8)	0.017
SUV_{peak}	3.7 (2.2–5.5)	2.4 (2.2–3.2)	0.050
MTV	3.3 (1.8–5.7)	2.1 (1.5–3.1)	0.055
TLG	9.9 (5.7–29.1)	5.0 (3.0–7.8)	0.002
MTV_{total}	27.4 (14.3–62.2)	18.0 (12.0–24.3)	0.040
TLG_{total}	54.2 (29.5–181.8)	36.0 (22.5–43.5)	0.026

Data are presented as the median (interquartile range). ^{18}F-FDG PET, fluorine-18 fluorodeoxyglucose positron emission tomography; PTLD, post-transplant lymphoproliferative disorder; SUV, standardized uptake value; MTV, metabolic tumor volume; TLG, total lesion glycolysis.

0.360–0.730) (see *Table 3*). The model is shown below.

By substituting the parameters in the model, we could distinguish between PTLD and non-PTLD patients. If a patient had digestive symptoms, the "digestive symptoms" factor in the model was equal to 1, if not, it was equal to 0. Other metabolic parameters could be calculated at the workstation. If the value of the model calculated was less than the cut-off value (of 0.77), the prediction result of the model was PTLD. The results of the comparisons between the model and each of the metabolic parameters that the model contained are summarized in *Table 4*. Based on the Delong test, the model had a significantly higher AUC than the SUV_{max} (Z=2.355, P=0.019), TLG (Z=2.118, P=0.034), and MTV_{total} (Z=2.181, P=0.029). Compared with the SUV_{max}, the IDI of combined model was 0.252 (95% CI: 0.110–0.394, P<0.001) and the NRI of combined model

Table 3 Differential diagnostic efficacies of the ^{18}F-FDG PET parameters and the different diagnostic models for distinguishing between PTLD and non-PTLD

Parameter	Cut-off	Accuracy (95% CI)	AUC (95% CI)	Sensitivity (95% CI)	Specificity (95% CI)	PPV (95% CI)	NPV (95% CI)
SUV_{max}	5.92	0.649 (0.511–0.771)	0.725 (0.597–0.853)	0.500 (0.341–0.659)	1.000 (0.771–1.000)	1.000 (0.800–1.000)	0.459 (0.299–0.629)
SUV_{mean}	3.17	0.649 (0.511–0.771)	0.701 (0.568–0.834)	0.550 (0.387–0.704)	0.882 (0.623–0.979)	0.917 (0.715–0.985)	0.455 (0.285–0.634)
SUV_{peak}	3.48	0.649 (0.511–0.771)	0.665 (0.518–0.813)	0.550 (0.387–0.704)	0.882 (0.623–0.979)	0.917 (0.715–0.985)	0.455 (0.285–0.634)
MTV	3.78	0.561 (0.424–0.693)	0.662 (0.523–0.800)	0.375 (0.232–0.542)	1.000 (0.771–1.000)	1.000 (0.747–1.000)	0.405 (0.260–0.567)
TLG	6.08	0.719 (0.585–0.830)	0.757 (0.632–0.883)	0.725 (0.559–0.849)	0.706 (0.440–0.886)	0.853 (0.682–0.945)	0.522 (0.311–0.726)
MTV_{total}	25.74	0.667 (0.529–0.786)	0.688 (0.549–0.827)	0.600 (0.434–0.747)	0.824 (0.558–0.953)	0.889 (0.697–0.971)	0.467 (0.288–0.654)
TLG_{total}	46.35	0.667 (0.529–0.786)	0.674 (0.536–0.812)	0.600 (0.434–0.747)	0.824 (0.558–0.953)	0.889 (0.697–0.971)	0.467 (0.288–0.654)
Model	0.77	0.754 (0.622–0.859)	0.868 (0.769–0.966)	0.675 (0.508–0.809)	0.941 (0.692–0.997)	0.964 (0.798–0.998)	0.552 (0.360–0.730)

Model: digestive symptoms plus SUV_{max} plus TLG plus MTV_{total}. ^{18}F-FDG PET, fluorine-18 fluorodeoxyglucose positron emission tomography; PTLD, post-transplant lymphoproliferative disorder; CI, confidence interval; AUC, area under the receiver operating characteristic curve; PPV, positive predictive value; NPV, negative predictive value; SUV, standardized uptake value; MTV, metabolic tumor volume; TLG, total lesion glycolysis.

Table 4 Comparison of the ^{18}F-FDG PET metabolic parameters and the different models according to the DeLong test, IDI, and NRI results

Variable	DeLong test		IDI			NRI		
	Z	P	Value	95% CI	P	Value	95% CI	P
Model *vs.* SUV_{max}	2.355	0.019	0.252	0.110–0.394	<0.001	0.628	0.240–1.016	0.002
Model *vs.* TLG	2.118	0.034	0.321	0.211–0.430	<0.001	0.697	0.356–1.038	<0.001
Model *vs.* MTV_{total}	2.181	0.029	0.331	0.191–0.472	<0.001	0.704	0.340–1.069	<0.001

Model: digestive symptoms plus SUV_{max} plus TLG plus MTV_{total}. ^{18}F-FDG PET, fluorine-18 fluorodeoxyglucose positron emission tomography/computerized tomography; IDI, integrated discrimination improvement; NRI, net reclassification improvement; CI, confidence interval; SUV, standardized uptake value; TLG, total lesion glycolysis; MTV, metabolic tumor volume.

was 0.628 (95% CI: 0.240–1.016, P=0.002); compared with TLG, the IDI was 0.321 (95% CI: 0.211–0.430, P<0.001) and the NRI of combined model was 0.697 (95% CI: 0.356–1.038, P<0.001); compared with the MTV_{total}, the IDI of combined model was 0.331 (95% CI: 0.191–0.472, P<0.001), the NRI of combined model was 0.704 (95% CI: 0.340–1.069, P<0.001). Thus, the model exhibited better differential diagnostic performance with multiparametric combination than metabolic parameters alone

Discussion

Our study showed that the ^{18}F-FDG PET/CT metabolic parameters could differentiate between PTLD and non-PTLD lymphadenopathy in pLT recipients with suspected PTLD. Further, diagnostic models based on ^{18}F-FDG PET metabolic parameters (i.e., SUV_{max}, TLG, and MTV_{total}) and clinical variables (i.e., digestive symptoms) can effectively help to differentiate between PTLD and non-PTLD lymphadenopathy.

It is still a challenge to differentiate PTLD from non-PTLD in pLT recipients. The clinical presentation of PTLD, including the nodal and extranodal disease, is non-specific and highly variable. Because of the abundant lymphoid tissues in the digestive system, the gastrointestinal tract is the most commonly affected organ among the extranodal organs (6,38). Therefore, PTLD needs to be considered in pLT recipients with unexplained digestive symptoms other than lymphadenopathy, such as abdominal pain, vomiting, and diarrhea (39,40). Radiographic assessment, which is non-invasive, is an important component of diagnosing PTLD (41). Ultrasound is the preferred initial non-invasive imaging examination; however, it may be greatly affected by intestinal gas (6). CT, which is another routine examination, is prone to missed diagnoses in cases with extranodal lesions (42). When chest involvement is suspected, magnetic resonance imaging is restricted by the small number of signal-generating protons due to the air in the lungs (43).

^{18}F-FDG PET/CT is a combination of CT and PET techniques that provides metabolic and anatomic information simultaneously. However, the use of PTLD in pediatric patients, particularly those who have undergone liver transplantation and subsequently developed PTLD, remains relatively limited. A variety of ^{18}F-FDG PET/CT parameters have been used to reflect the metabolic activity of the target VOI. The SUV_{max}, which is defined as the maximum uptake value among the VOI, is the most widely used parameter due to its simplicity and repeatability. In our study, the SUV_{max} had high specificity but low sensitivity. The discriminatory value of the SUV_{max} has been also reported by Si *et al.* (44). However, the SUV_{max} does not represent the metabolism of the whole lesion and may be disturbed by various factors, such as image noise, statistical fluctuation, and partial volume effect (45).

As a volumetric parameter, the MTV represents the volume of cells with high glycolytic activity, while TLG reflects both the volume and activity, and thus provides a better measure of the whole tumor metabolic activity (46). In our study, TLG had moderate differential diagnostic ability (AUC =0.757), which shows the discrimination value of the volumetric parameters. Due to the clinical characteristics of PTLD in pLT, we also evaluated the condition of systemic lesions by ^{18}F-FDG PET/CT. By summing the MTV and TLG of all target lesions, the MTV_{total} and TLG_{total}, which are indicators of whole-body tumor burden and have been proven valuable in predicting prognosis and evaluating treatment efficacy, were then calculated (47). However, the discriminatory performance of the MTV_{total} (AUC =0.688) and TLG_{total} (AUC =0.674) were not satisfactory. This may be due to the lower metabolic activity of some PTLD lesions, which is similar to that of

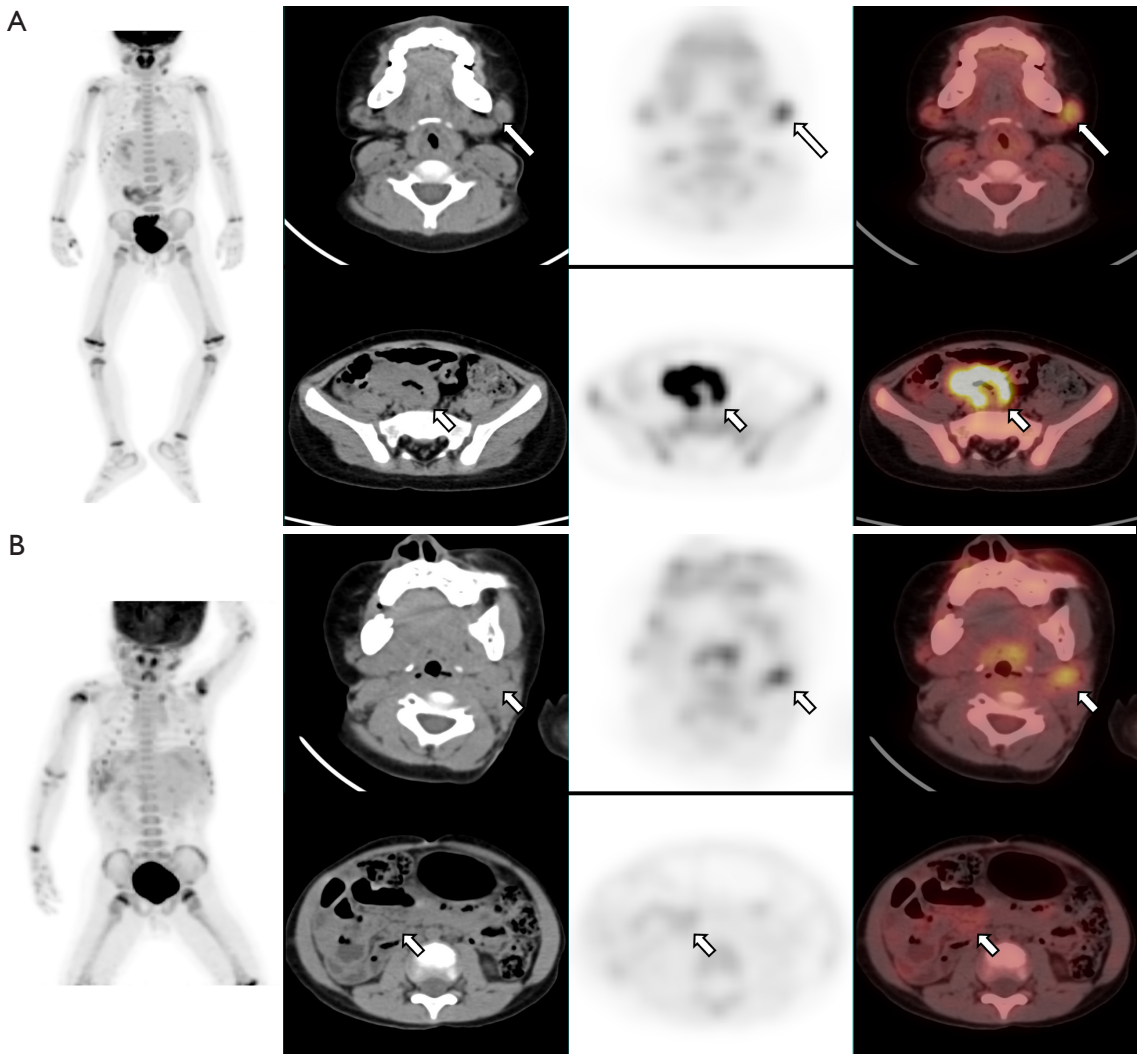

Figure 2 PTLD and non-PTLD lymphadenopathy in pLT recipients. (A) PTLD case. A 4-year-old boy presented with abdominal pain and lymphadenopathy 3 years after pLT for biliary atresia. The key findings of the ^{18}F-FDG PET/CT were as follows. First, the posterior wall of the nasopharynx was thickened with abnormal ^{18}F-FDG uptake. Second, the cervical lymph nodes were enlarged with abnormal ^{18}F-FDG uptake (long arrow). Third, the small bowel wall was thickened focally with abnormal ^{18}F-FDG uptake. A small bowel resection was performed, and the results showed monomorphic PTLD (short arrow). (B) Non-PTLD lymphadenopathy. A 2-year-old boy presented with lymphadenopathy alone 2 years after pLT for biliary atresia. The key findings of the ^{18}F-FDG PET/CT were as follows. First, the posterior wall of the nasopharynx was thickened with abnormal ^{18}F-FDG uptake. Second, the cervical and retroperitoneal lymph nodes were enlarged with abnormal ^{18}F-FDG uptake (short arrow). A cervical lymph node biopsy was performed, and the results showed reactive hyperplasia (short arrow). PTLD, post-transplant lymphoproliferative disorder; pLT, pediatric liver transplantation; ^{18}F-FDG PET, fluorine-18 fluorodeoxyglucose positron emission tomography.

non-PTLD lesions. Therefore, the application of a single metabolic parameter of ^{18}F-FDG PET/CT may not provide assistance in providing differential diagnoses.

Due to the limitations of any single parameter in providing effective differential diagnosis capabilities, we integrated the clinical characteristics and metabolic parameters to construct a diagnostic model. The model combined clinical characteristics (i.e., digestive symptoms), the metabolic parameters of single lesions (i.e., the SUV_{max} and TLG), and the systemic metabolic status of the patients

(i.e., the MTV_{total}) (*Figure 2*). The IDI and Delong test results showed that the combination model had a higher diagnostic efficacy (AUC =0.868) than any of the metabolic parameters alone, and moderate sensitivity (0.675) and high specificity (0.941). To our knowledge, our study is the first to establish a diagnostic model for discriminating between PTLD and non-PTLD lymphadenopathy.

This study had some limitations. First, this study conducted a retrospective analysis at a single center with a limited sample size. Second, as this was a retrospective study, many parameters that may be helpful for diagnosis, such as lactate dehydrogenase and levels of inflammatory proteins (interleukin 6 or interleukin 10), were not included (24). In the future, we will add additional parameters to enhance the discriminative power of our model. Third, while we had strict standards for the diagnosis of PTLD and non-PTLD lesions, there is still a possibility of omission or overdiagnosis, especially for PTLD patients, which might have led to a bias. Based on these limitations, it is recommended that a multi-center prospective study with a larger sample size be conducted in the future to further investigate this topic.

In conclusion, our study found that ^{18}F-FDG PET/CT is an efficient technique for the differential diagnosis between PTLD and non-PTLD lymphadenopathy in pLT recipients. Among the multiple parameters examined, TLG was the most effective parameter. The diagnostic model that combined clinical characteristics and metabolic parameters showed excellent performance in the differential diagnosis of PTLD and non-PTLD lymphadenopathy. Our results might improve the diagnosis of PTLD in pLT recipients and result in fewer children having to undergo unnecessary invasive examinations and treatments.

Acknowledgments

Funding: This study was supported by grants from Beijing Municipal Natural Science Foundation (No. 7232031) and National Natural Science Foundation of China (No. 82272034).

Footnote

Reporting Checklist: The authors have completed the STARD reporting checklist. Available at https://qims.amegroups.com/article/view/10.21037/qims-23-1059/rc

Conflicts of Interest: All authors have completed the ICMJE uniform disclosure form (available at https://qims.amegroups.com/article/view/10.21037/qims-23-1059/coif). The authors have no conflicts of interest to declare.

Ethical Statement: The authors are accountable for all aspects of the work in ensuring that questions related to the accuracy or integrity of any part of the work are appropriately investigated and resolved. The study was conducted in accordance with the Declaration of Helsinki (as revised in 2013). The study was approved by the Research Ethics Committee of the Beijing Friendship Hospital, Capital Medical University, and the requirement of individual consent for this retrospective analysis was waived.

References

1. Absalon MJ, Khoury RA, Phillips CL. Post-transplant lymphoproliferative disorder after solid-organ transplant in children. Semin Pediatr Surg 2017;26:257-66.
2. Lauro A, Arpinati M, Pinna AD. Managing the challenge of PTLD in liver and bowel transplant recipients. Br J Haematol 2015;169:157-72.
3. Hsu CT, Chang MH, Ho MC, Chang HH, Lu MY, Jou ST, Ni YH, Chen HL, Hsu HY, Wu JF. Post-transplantation lymphoproliferative disease in pediatric liver recipients in Taiwan. J Formos Med Assoc 2019;118:1537-45.
4. Lindsay J, Othman J, Heldman MR, Slavin MA. Epstein-Barr virus posttransplant lymphoproliferative disorder: update on management and outcomes. Curr Opin Infect Dis 2021;34:635-45.
5. Okamoto T, Okajima H, Uebayashi EY, Ogawa E, Yamada Y, Umeda K, Hiramatsu H, Hatano E. Management of Epstein-Barr Virus Infection and Post-Transplant Lymphoproliferative Disorder in Pediatric Liver Transplantation. J Clin Med 2022;11:2166.
6. Marie E, Navallas M, Navarro OM, Punnett A, Shammas

A, Gupta A, Chami R, Shroff MM, Vali R. Posttransplant Lymphoproliferative Disorder in Children: A 360-degree Perspective. Radiographics 2020;40:241-65.
7. Rosenberg TL, Nolder AR. Pediatric cervical lymphadenopathy. Otolaryngol Clin North Am 2014;47:721-31.
8. Spijkers S, Littooij AS, Nievelstein RAJ. Measurements of cervical lymph nodes in children on computed tomography. Pediatr Radiol 2020;50:534-42.
9. Kim JW, Baek JY, Lee JY, Lim SM, Kang JM, Ahn WK, Hahn SM, Han JW, Lyu CJ, Ahn JG. Pathologic etiology and predictors of malignancy in children with cervical lymphadenopathy. World J Pediatr 2023;19:283-7.
10. Faraz M, Rosado FGN. Reactive Lymphadenopathies. Clin Lab Med 2021;41:433-51.
11. Zaffiri L, Chambers ET. Screening and Management of PTLD. Transplantation 2023;107:2316-28.
12. Allen UD, Preiksaitis JK; AST Infectious Diseases Community of Practice. Post-transplant lymphoproliferative disorders, Epstein-Barr virus infection, and disease in solid organ transplantation: Guidelines from the American Society of Transplantation Infectious Diseases Community of Practice. Clin Transplant 2019;33:e13652.
13. Perito ER, Martinez M, Turmelle YP, Mason K, Spain KM, Bucuvalas JC, Feng S. Posttransplant biopsy risk for stable long-term pediatric liver transplant recipients: 451 percutaneous biopsies from two multicenter immunosuppression withdrawal trials. Am J Transplant 2019;19:1545-51.
14. Ilivitzki A, Sokolovski B, Assalia A, Benbarak A, Postovsky S, Glozman L, Ben-Arush M. Ultrasound-Guided Core Biopsy for Tissue Diagnosis in Pediatric Oncology: 16-Year Experience With 597 Biopsies. AJR Am J Roentgenol 2021;216:1066-73.
15. Zhao D, Zhou T, Luo Y, Wu C, Xu D, Zhong C, Cong W, Liu Q, Zhang J, Xia Q. Preliminary clinical experience applying donor-derived cell-free DNA to discern rejection in pediatric liver transplant recipients. Sci Rep 2021;11:1138.
16. Ruijter BN, Wolterbeek R, Hew M, van Reeven M, van der Helm D, Dubbeld J, Tushuizen ME, Metselaar H, Vossen ACTM, van Hoek B. Epstein-Barr Viral Load Monitoring Strategy and the Risk for Posttransplant Lymphoproliferative Disease in Adult Liver Transplantation : A Cohort Study. Ann Intern Med 2023;176:174-81.
17. Kedi W, Dongjiang X, Zhi L, Yan G, Kun J, Jianrong S. The rational specimen for the quantitative detection of Epstein-Barr virus DNA load. Clin Chem Lab Med 2019;57:759-65.
18. Kanakry JA, Hegde AM, Durand CM, Massie AB, Greer AE, Ambinder RF, Valsamakis A. The clinical significance of EBV DNA in the plasma and peripheral blood mononuclear cells of patients with or without EBV diseases. Blood 2016;127:2007-17.
19. Kimura H, Kwong YL. EBV Viral Loads in Diagnosis, Monitoring, and Response Assessment. Front Oncol 2019;9:62.
20. Dharnidharka VR. Peripheral Blood Epstein-Barr Viral Nucleic Acid Surveillance as a Marker for Posttransplant Cancer Risk. Am J Transplant 2017;17:611-6.
21. Allen UD, Preiksaitis JK; AST Infectious Diseases Community of Practice. Epstein-Barr virus and posttransplant lymphoproliferative disorder in solid organ transplantation. Am J Transplant 2013;13 Suppl 4:107-20.
22. Song H, Guja KE, Iagaru A. (18)F-FDG PET/CT for Evaluation of Post-Transplant Lymphoproliferative Disorder (PTLD). Semin Nucl Med 2021;51:392-403.
23. Metser U, Lo G. FDG-PET/CT in abdominal post-transplant lymphoproliferative disease. Br J Radiol 2016;89:20150844.
24. Montes de Jesus FM, Kwee TC, Kahle XU, Nijland M, van Meerten T, Huls G, Dierckx RAJO, Rosati S, Diepstra A, van der Bij W, Verschuuren EAM, Glaudemans AWJM, Noordzij W. Diagnostic performance of FDG-PET/CT of post-transplant lymphoproliferative disorder and factors affecting diagnostic yield. Eur J Nucl Med Mol Imaging 2020;47:529-36.
25. Montes de Jesus FM, Glaudemans AWJM, Tissing WJ, Dierckx RAJO, Rosati S, Diepstra A, Noordzij W, Kwee TC. (18)F-FDG PET/CT in the Diagnostic and Treatment Evaluation of Pediatric Posttransplant Lymphoproliferative Disorders. J Nucl Med 2020;61:1307-13.
26. Feng L, Yang X, Lu X, Wang W, Yang J. Solitary Central Nervous System Relapse of Posttransplant Lymphoproliferative Disorder on 18 F-FDG PET/CT. Clin Nucl Med 2022;47:1007-9.
27. Xu YF, Yang JG. Roles of F-18-Fluoro-2-Deoxy-Glucose PET/Computed Tomography Scans in the Management of Post-Transplant Lymphoproliferative Disease in Pediatric Patient. PET Clin 2020;15:309-19.
28. Lu X, Kan Y, Wang W, Yang J. Primary Cutaneous Natural Killer/T-Cell Lymphoma: A Posttransplant Lymphoproliferative Disorder Demonstrated by 18F-FDG

PET/CT. Clin Nucl Med 2021;46:595-8.
29. Brown AK, Carapellucci J, Oshrine B, Gomez A, Meoded A, Asante-Korang A. Diagnostic and management roles of FDG PET/CT imaging in post-transplant lymphoproliferation in pediatric heart transplantation. Clin Transplant 2023;37:e15015.
30. Van Keerberghen CA, Goffin K, Vergote V, Tousseyn T, Verhoef G, Laenen A, Vandenberghe P, Dierickx D, Gheysens O. Role of interim and end of treatment positron emission tomography for response assessment and prediction of relapse in posttransplant lymphoproliferative disorder. Acta Oncol 2019;58:1041-7.
31. Panagiotidis E, Quigley AM, Pencharz D, Ardeshna K, Syed R, Sajjan R, Bomanji J. (18)F-fluorodeoxyglucose positron emission tomography/computed tomography in diagnosis of post-transplant lymphoproliferative disorder. Leuk Lymphoma 2014;55:515-9.
32. Kim JH, Cho H, Sung H, Jung AR, Lee YS, Lee SW, Ryu JS, Chae EJ, Kim KW, Huh J, Park CS, Yoon DH, Suh C. Reappraisal of the prognostic value of Epstein-Barr virus status in monomorphic post-transplantation lymphoproliferative disorders-diffuse large B-cell lymphoma. Sci Rep 2021;11:2880.
33. Markouli M, Ullah F, Omar N, Apostolopoulou A, Dhillon P, Diamantopoulos P, Dower J, Gurnari C, Ahmed S, Dima D. Recent Advances in Adult Post-Transplant Lymphoproliferative Disorder. Cancers (Basel) 2022.
34. Adams HJ, de Klerk JM, Fijnheer R, Heggelman BG, Dubois SV, Nievelstein RA, Kwee TC. Prognostic superiority of the National Comprehensive Cancer Network International Prognostic Index over pretreatment whole-body volumetric-metabolic FDG-PET/CT metrics in diffuse large B-cell lymphoma. Eur J Haematol 2015;94:532-9.
35. Boellaard R, Delgado-Bolton R, Oyen WJ, Giammarile F, Tatsch K, Eschner W, et al. FDG PET/CT: EANM procedure guidelines for tumour imaging: version 2.0. Eur J Nucl Med Mol Imaging 2015;42:328-54.
36. Montes de Jesus F, Dierickx D, Vergote V, Noordzij W, Dierckx RAJO, Deroose CM, Glaudemans AWJM, Gheysens O, Kwee TC. Prognostic superiority of International Prognostic Index over [18F]FDG PET/CT volumetric parameters in post-transplant lymphoproliferative disorder. EJNMMI Res 2021;11:29.
37. Albano D, Bosio G, Pagani C, Re A, Tucci A, Giubbini R, Bertagna F. Prognostic role of baseline 18F-FDG PET/CT metabolic parameters in Burkitt lymphoma. Eur J Nucl Med Mol Imaging 2019;46:87-96.
38. Takehana CS, Twist CJ, Mosci C, Quon A, Mittra E, Iagaru A. (18)F-FDG PET/CT in the management of patients with post-transplant lymphoproliferative disorder. Nucl Med Commun 2014;35:276-81.
39. Cao S, Cox K, Esquivel CO, Berquist W, Concepcion W, Ojogho O, Monge H, Krams S, Martinez O, So S. Posttransplant lymphoproliferative disorders and gastrointestinal manifestations of Epstein-Barr virus infection in children following liver transplantation. Transplantation 1998;66:851-6.
40. Rao S, Smith DA, Kikano EG, Tirumani SH, Beck R, Ramaiya NH. Posttransplant Lymphoproliferative Disorder Status Post-Solid Organ Transplant Presenting to the Emergency Department: Single Institute Experience. J Comput Assist Tomogr 2021;45:894-903.
41. Dharnidharka VR, Webster AC, Martinez OM, Preiksaitis JK, Leblond V, Choquet S. Post-transplant lymphoproliferative disorders. Nat Rev Dis Primers 2016;2:15088.
42. Dierickx D, Tousseyn T, Requilé A, Verscuren R, Sagaert X, Morscio J, Wlodarska I, Herreman A, Kuypers D, Van Cleemput J, Nevens F, Dupont L, Uyttebroeck A, Pirenne J, De Wolf-Peeters C, Verhoef G, Brepoels L, Gheysens O. The accuracy of positron emission tomography in the detection of posttransplant lymphoproliferative disorder. Haematologica 2013;98:771-5.
43. Ball L, Braune A, Spieth P, Herzog M, Chandrapatham K, Hietschold V, Schultz MJ, Patroniti N, Pelosi P, Gama de Abreu M. Magnetic Resonance Imaging for Quantitative Assessment of Lung Aeration: A Pilot Translational Study. Front Physiol 2018;9:1120.
44. Si Z, Lu D, Zhai L, Zheng W, Dong C, Sun C, Wang K, Zhang W, Wei X, Zhang Z, Zhao S, Gao W, Shen Z. The value of (18) F-FDG PET/CT quantitative indexes in the diagnosis of nondestructive posttransplant lymphoproliferative disorders after pediatric liver transplantation. Pediatr Transplant 2023;27:e14501.
45. Akamatsu G, Ikari Y, Nishida H, Nishio T, Ohnishi A, Maebatake A, Sasaki M, Senda M. Influence of Statistical Fluctuation on Reproducibility and Accuracy of SUVmax and SUVpeak: A Phantom Study. J Nucl Med Technol 2015;43:222-6.
46. Im HJ, Bradshaw T, Solaiyappan M, Cho SY. Current Methods to Define Metabolic Tumor Volume in Positron Emission Tomography: Which One is Better? Nucl Med Mol Imaging 2018;52:5-15.

47. Lawal IO, Lengana T, Janse van Rensburg C, Reyneke F, Popoola GO, Ankrah AO, Sathekge MM. Fluorodeoxyglucose Positron Emission Tomography integrated with computed tomography in carcinoma of the cervix: Its impact on accurate staging and the predictive role of its metabolic parameters. PLoS One 2019;14:e0215412.

Cite this article as: Wang C, Wang G, Wang W, Kan Y, Zhang M, Yang J. The role of ^{18}F-FDG PET/CT metabolic parameters in the differential diagnosis of post-transplant lymphoproliferative disorder after pediatric liver transplantation. Quant Imaging Med Surg 2024;14(2):1323-1334. doi: 10.21037/qims-23-1059

